

# First direct astrophysical constraints on dark matter interactions with ordinary matter at very low velocities

Digvijay Wadekar\* and Glennys R. Farrar†

Center for Cosmology and Particle Physics, Department of Physics,  
New York University, New York, NY 10003, USA

(Dated: March 26, 2019)

We derive the first direct constraints on dark matter cross sections at very low velocity,  $v \approx 10$  km/s, by requiring that the heating/cooling due to DM interacting with gas in the Leo T dwarf galaxy not exceed the radiative cooling rate of the gas. This gives strong direct limits on millicharged DM with mass  $\lesssim 1$  GeV, which close important gaps in the exclusion plots and add to constraints on the recent EDGES 21 cm absorption anomaly. We also set new bounds on ultra-light dark photon DM and on DM-electron interactions. Combining equilibrium heating/cooling constraints from Leo T and robust Galactic gas clouds, we improve the constraints on DM-baryon cross-sections for arbitrary velocity dependences.

The particle nature of Dark Matter (DM) and its origin is still a mystery. Recently, the EDGES collaboration reported observations suggesting the temperature of gas during the cosmic dawn of the Universe was roughly half the expected value [1]. To explain the anomalous observation, Ref. [2] proposed that DM exchanges heat with the HI gas by non-standard Coulomb-like interactions of the form  $\sigma \propto v_{\text{rel}}^{-4}$  between DM and baryons. A physically motivated model that can lead to Coulomb-like DM gas interactions is the millicharged model [3]. Because the relative velocity between DM and baryons at the cosmic dawn is much lower than in standard astrophysical systems ( $v_{\text{rel}} \lesssim 0.3$  km/s), the explanation by [2] is effective at heating the gas during the cosmic dawn and simultaneously evading the traditional astrophysical bounds on DM.

With the exception of [4] which pertains exclusively to masses near 1 GeV, existing astrophysical constraints are obtained from systems with high  $v_{\text{rel}} \gtrsim 300$  km/s and then extrapolated to low  $v_{\text{rel}}$  assuming a power law velocity dependence. However, such an extrapolation is invalid if the assumed power law dependence on  $v_{\text{rel}}$  does not hold over the entire range. In this paper, we use the well-studied gas-rich dwarf galaxy Leo T with a low baryon velocity dispersion  $v_{\text{HI}} \sim 7$  km/s [5–7]. We require that the DM heating/cooling rate not exceed the radiative cooling rate of the HI gas in Leo T and therefore obtain the first *direct* constraints at low velocity on DM-gas interactions. Our constraints are complementary to the early universe constraints on millicharged DM [8–14], because the Leo T constraints make no assumptions about cosmology.

In addition to using Leo T to improve the constraints on DM interactions in the cosmic dawn and on millicharged DM more generally, we report constraints on DM-baryon interaction cross-sections of the form  $\sigma \propto v_{\text{rel}}^n$  using gas clouds in the Milky Way (MW). The use of MW gas clouds for constraining DM was proposed by Bhoonah *et al.* [15] (B18 below). MW systems can be more sensitive than Leo T to DM heat exchange in parts of the

parameter range, especially for  $n > -2$ , because the relative velocity between gas and DM is characterized by the much higher virial velocity of DM in the MW halo, leading to a higher energy transfer rate. However B18 chose clouds discovered by [16] which are entrained in the hot, high-velocity nuclear outflow (HVNO) — a stream of gas at  $T \sim 10^{6-7}$  K moving at  $\sim 330$  km/s outward from the Galactic Center [16, 17]. Clouds in such an extreme environment cannot be assumed to be stable over the long timescales associated with their radiative cooling rates. The clouds are subject to a number of destructive effects due to their environment [18–22], some of which occur at comparatively much shorter timescales; see Supplemental Materials [23] (SM) for further details. Therefore, we eschew use of the HVNO clouds and instead use the robustly observed gas clouds of [24] which are in tranquil environments co-rotating with the galactic disk and not close to the Galactic center.

A crucial feature of Leo T and certain MW gas clouds making them suitable for constraining DM-gas interactions is their low astrophysical radiative cooling rates. This makes them more sensitive to energy transfer by a non-standard thermal source. The radiative cooling rate of HI gas increases as the temperature, density, or metallicity of the gas increases; Leo T has low metallicity and the MW gas clouds that we analyze are cold ( $T < 500$  K). In Leo T, the heat exchange between DM and gas is similar to that in a system of two fluids in thermal contact. Instead, in MW gas clouds, there is a high relative bulk velocity between the two fluids. In addition to the standard thermal energy exchange, DM-gas interactions produce an additional friction force to damp the relative velocity which also heats the gas in clouds.

## Thermal Equilibrium bounds

In an astrophysical system, let  $\dot{Q} = \frac{dE}{dtdV}$  be the volumetric energy transfer rate due to collisions of DM with

gas particles of type  $i$  (electrons, ions or atomic nuclei):

$$\dot{Q} = \sum_i \int d^3v_i f(v_i) \int d^3v_\chi f(v_\chi) n_i n_\chi v_{\text{rel}} E_T(v_{\text{rel}}) \sigma_{i\chi}^T, \quad (1)$$

where  $n$  is the number density,  $f(v)$  is the velocity distribution,  $E_T(v_{\text{rel}})$  is the energy transferred in the DM scattering,  $\sigma_{i\chi}^T$  is the cross section. Let  $\dot{C}$  and  $\dot{H}$  be the volumetric radiative cooling rate and the astrophysical heating rate, respectively. For a system to be in thermal equilibrium, we need  $|\dot{Q}| = |\dot{C} - \dot{H}|$ . In this paper, we set conservative bounds on the DM interaction cross section by requiring  $|\dot{Q}| \leq |\dot{C}|$ . More stringent bounds can be placed by including the astrophysical heating rate  $|\dot{Q}| \leq |\dot{C} - \dot{H}|$ ; see SM [23] for a discussion.

Radiative cooling— To compute  $\dot{C}$  for HI gas in Leo T and the MW clouds, we use

$$\dot{C} = n_{\text{H}}^2 \Lambda(T), \quad (2)$$

where  $n_{\text{H}}$  is the hydrogen number density and  $\Lambda(T)$  is the cooling function which depends on the temperature and metallicity of the gas. We obtain  $\Lambda(T)$  from the astrophysical radiative cooling library Grackle [25]. The cooling function scales with metallicity of HI gas as  $\Lambda(T) \propto 10^{[\text{Fe}/\text{H}]}$  where the metallicity is defined as:  $[\text{Fe}/\text{H}] \equiv \log_{10}(n_{\text{Fe}}/n_{\text{H}})_{\text{gas}} - \log_{10}(n_{\text{Fe}}/n_{\text{H}})_{\text{Sun}}$ ; see SM [23] for further details.

### Properties of astrophysical systems used

Leo T galaxy— Leo T is an ultra-faint dwarf irregular galaxy located about 420 kpc from the Milky Way. It is the most dark-matter dominated dwarf in the Local Group and is also gas-rich, which makes it a unique astrophysical system to study DM scattering effects. Moreover Leo T is well-studied observationally and has garnered modelling attention. The kinematics of Leo T are well measured using both stars and gas; the velocity dispersion is  $v_{\text{H}_1} \sim 7$  km/s ( $T \simeq 6000$ K) [5–7]. Ref. [5] analyzed high-resolution Giant Meterwave Radio Telescope (GMRT) and Westerbork Synthesis Radio Telescope (WSRT) observations to determine the HI gas distribution. Ref. [26] found the mean spectroscopic metallicity to be  $[\text{Fe}/\text{H}] \sim -1.99 \pm 0.05$  [27], so Leo T is metal poor (like the majority of ultra-faint dwarfs) and we need only consider H and He with the cosmic density fraction  $n_{\text{He}}/n_{\text{H}} = 0.08$  for calculating DM-gas interactions.

Ref. [28] modelled the DM halo of Leo T by fitting an isothermal DM profile to the HI distribution of [5], taking account of the metagalactic background as necessary for interpreting the HI column density profile and determining the distribution of free electrons; see also [29]. We adopt the model of [28] for our analysis and show the individual components in this model in Fig.

1. A comprehensive modeling effort including the latest observations of [7] and utilizing the iterative-unfolding

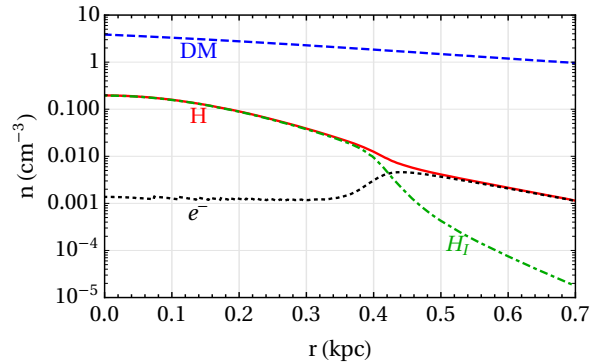


FIG. 1. Number density of DM (for  $m_\chi = 1$  GeV), atomic hydrogen (HI), electrons ( $e^-$ ) and total hydrogen (H) components of Leo T given by the model of [28].

technique of [30], while also modeling the metagalactic ionization profile and known astrophysical heating and cooling, will result in a yet better description of Leo T and enable more accurate determination of the limits on DM interactions using this system.

There is no evidence of coherent rotation in Leo T, and low-mass dwarf galaxies like Leo T as a class do not exhibit rotation [31], so we can discount the possibility of coherent rotation which eludes detection because  $\hat{J}$  is along our line of sight. The baryons and DM of Leo T move in the same gravitational potential and since there is no other significant source of support for the gas, the velocity dispersion of the gas and DM must be equal ( $v_\chi = v_{\text{H}_1}$ ). As a result, DM heats or cools the gas depending on the DM-proton mass difference because  $T_\chi - T_{\text{H}_1} = (m_\chi - m_p)v_{\text{H}_1}^2/2$ ;  $T_{\text{He}} = T_{\text{H}}$  due to the large atomic cross-section.

The outer part of Leo T ( $r > 0.35$  kpc) is ionized. It is difficult to find a robust measure of the rate at which the outer ionized region cools. Therefore, we restrict our study to the inner region  $0 < r < 0.35$  kpc (designated *Region-1* below), which is largely un-ionized and shielded from the metagalactic UV background; see also [32]. For calculating the thermal equilibrium bound in Leo T, we integrate the volumetric radiative cooling rate and the DM energy transfer rate over Region-1 and then require  $|\int_{\text{Region-1}} \dot{Q} dV| \leq |\int_{\text{Region-1}} \dot{C} dV|$ . The average value of  $\dot{C}$  for gas in Leo T in Region-1 is  $\sim 2.1 \times 10^{-30}$  erg cm $^{-3}$  s $^{-1}$ .

Milky Way gas clouds—We use cores of high Galactic latitude clouds which were observed with both the Very Large Array (VLA) and the Green Banks Telescope (GBT) [24]. These clouds are co-rotating with the MW disk and their mean velocity relative to DM is 220 km/s [33–35]. These clouds are at a distance 0.4–1 kpc from the disk and are considered to be representative of typical clouds and to have near-solar metallicities [36–40].

Among the co-rotating clouds in [24], we find that the core of the G33.4–8.0 cloud gives the strongest constraint

on DM interactions and the best gas cloud bounds reported in this paper are derived from it; other clouds give similar bounds, as shown in the SM [23]. G33.4–8.0 has the following parameters:  $n_{\text{HI}} = 0.4 \pm 0.1 \text{ cm}^{-3}$ ,  $T = 400 \pm 90 \text{ K}$ ,  $R = 4.68 \pm 0.41 \text{ kpc}$  and  $z = -1 \pm 0.28 \text{ kpc}$  where  $R, z$  are cylindrical coordinates with origin at the Galactic center [24]. The value of  $\dot{C}$  for gas in G33.4–8.0 is  $\sim 2.1 \times 10^{-27} \text{ erg cm}^{-3} \text{ s}^{-1}$ . To find its local DM density we adopt the NFW profile  $\rho_\chi = \rho_0 / [(r/r_0)(1+r/r_0)^2]$  with  $\rho_0 = 0.32 \text{ GeV/cm}^3$ , scale radius  $r_0 = 16 \text{ kpc}$  and virial radius 180 kpc for the Milky Way DM halo from [41]. Using the best-fit Burkert profile from [42] gives a similar but slightly higher value, so the NFW choice is conservative. We adopt an isotropic DM velocity dispersion profile from [43]. The DM density and velocity dispersion at the location of G33.4–8.0 thus derived are  $0.64 \text{ GeV/cm}^3$  and  $124.4 \text{ km/s}$  respectively.

### DM heat exchange

In Leo T, the heat exchange by DM-gas interactions is similar to a system of two fluids with different temperatures in thermal contact without any relative bulk velocity between them. For DM mass above (below) the proton mass, the DM heats (cools) the HI gas because the temperature difference between DM and HI is  $T_\chi - T_{\text{HI}} = (m_\chi - m_p)v_{\text{HI}}^2/2$ .

In the case of MW clouds, the situation is different from Leo T because in addition to the velocity dispersion there is a high relative bulk velocity (220 km/s) between the gas and DM which leads to frictional heating of the two fluids. The energy transferred to a particle  $i$  in the cloud by a DM collision is  $E_T = \mu_{i\chi}^2 v_{\text{rel}}^2 (1 - \theta_{\text{CM}})/m_i$ , where  $\mu_{i\chi}$  is the DM-particle reduced mass and  $\theta_{\text{CM}}$  is the scattering angle in the center of mass frame. See the SM [23] for the formalism of heat exchange in Leo T and gas clouds.

Millicharge model— In the millicharged DM model [3] the DM particle effectively carries a small electric charge  $Q = \epsilon e$ , where  $e$  is the charge on an electron. Such a model naturally leads to Coulomb-like DM-gas interactions  $\sigma \propto v_{\text{rel}}^{-4}$ . There are two possibilities for the origin of such DM-gas interactions: a light  $U(1)$  gauge boson (hidden photon) kinematically mixed with the Standard Model photon, or DM particle carrying a tiny charge. Our constraints are applicable for both scenarios.

There are two ways in which charged DM particles can interact with the Leo T galaxy and the MW clouds. The first is that the DM particles interact with free electrons and ions. As shown in Fig. 1 for Leo T, a fraction of Hydrogen is ionized even in Region-1 because of penetrating metagalactic background. The MW cloud cores we use are at comparatively lower temperatures, so we conservatively consider that only carbon, silicon and iron in the clouds are ionized by the metagalactic background [44, 45]. The second scenario arises when the de Broglie

wavelength of DM becomes smaller than the screening length of the atom. Charged DM can then interact with the nucleus  $A$  of neutral atoms in the astrophysical systems for nuclear recoil energy  $E_{\text{nr}} \gtrsim 1/(2m_A a_0^2)$  because the nucleus is screened over a distance  $\sim a_0$  (Bohr radius). For DM in Leo T interacting with the Hydrogen nucleus, this happens for  $m_\chi \gtrsim 0.07 \text{ GeV}$ . The number density of neutral atoms in Leo T is enough greater than that of electrons or ions, that the dominant contribution to heat exchange by DM for  $m_\chi \gtrsim 0.07 \text{ GeV}$  comes from neutral H and He atoms.

## Results

The most basic Leo T constraint on DM-gas interactions comes from the very existence of its DM halo. If  $m_\chi < m_p$  and the DM-gas interactions are frequent enough, DM would evaporate rather than remaining gravitationally bound. On the other hand, if  $m_\chi > m_p$  and the interactions are strong enough, the DM profile would be visibly more concentrated than observed due to being cooled by its interactions with gas. Proper evaluation of these constraints requires simultaneously modeling the DM and gas distributions which we leave for the future. In lieu of that, we indicate with the dashed gray line of Fig. 2, the value of  $\epsilon$  such that the characteristic DM energy loss/gain time is more than the Leo T lifetime,  $(d\ln E/dt)^{-1} \approx 10 \text{ Gyr}$ .

Our stronger constraints from the observed temperature of the HI gas in Leo T are shown by the black solid line in Fig. 2. This limit lies below the grey line, so gas cooling/heating rather than DM evaporation/collapse is the dominant effect. The Leo T temperature constraints are weakest for DM mass close to 1 GeV, where DM and gas are at similar temperatures and there is no heat exchange. This is precisely the DM mass regime for which Earth can have a significant DM atmosphere and the results of [4] apply. Translating the constraints of [4] into the  $\epsilon - m_\chi$  parameter space is non-trivial, but is underway [46]. Fig. 2 also shows constraints taken from [47, 48] provided by the SLAC millicharge experiment [49], SENSEI [48], XENON10 [50, 51], XQC Rocket [52] and CRESST Surface Run (CSR) [53]. The dashed cyan line labeled as CMB is our translation of the DM-proton interaction cross section limits of [10]. The XQC and CSR exclusion regions [47] assume a nuclear recoil thermalization efficiency of 2% and are merely suggestive of the bounds that may be possible, because the efficiency must be calibrated experimentally [47].

The largest uncertainty in our Leo T bounds comes from the uncertainty in the DM and gas densities and the HI ionization fraction profile, as discussed above. An estimate of the maximum weakening that could occur can be obtained using the DM and HI distributions of [30] along with the ionization model of [28]; this changes the limit on  $\epsilon$  by less than a factor-2. A more detailed treat-

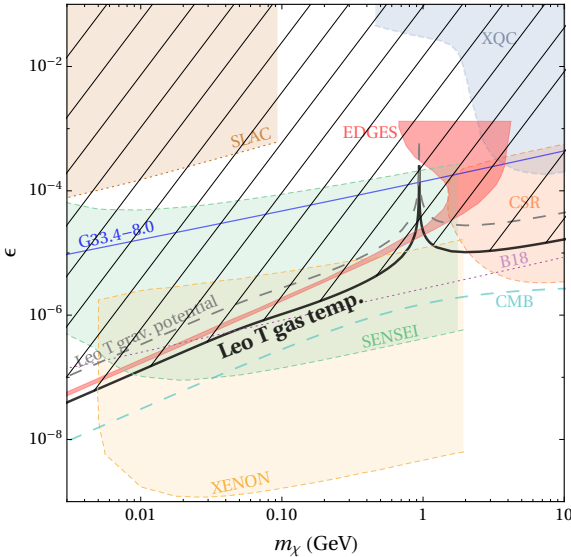


FIG. 2. Upper bound on the charge of DM from the Leo T galaxy (black); these constraints can be extrapolated to the left and right using  $\epsilon_{\max} \sim 10^{-4.9}(m/\text{GeV})$  and  $\epsilon_{\max} \sim 10^{-5.3}\sqrt{(m/\text{GeV})}$ . The dashed grey line indicates the approximate value above which the DM halo itself could be modified due to evaporation or collapse. The blue line shows the upper bound from the best MW co-rotating gas cloud, G33.4–8.0, while the (invalid) constraint reported by B18 is shown by the purple dotted line; see SM [23] for details. We show in red the parameter range which explains the EDGES 21cm anomaly taken from [54] (see also [11, 55, 56]). Note that the Leo T bounds cannot be trivially extrapolated for the case when a fraction of DM is charged; see text for details and for the other constraints shown.

ment that balances the identifiable astrophysical heating and cooling could enable stronger limits to be set as discussed above. This requires modeling the observed HI luminosity and temperature profiles self-consistently with the DM distribution including the effects of astrophysical heating and cooling along with possible heating or cooling due to DM-gas interactions. Such self-consistent modeling will map out more precisely the constraints imposed by the existence of the observed gravitational potential, possibly identifying parameters of a sub-component of light DM whose interactions with gas cause it to evaporate and thereby evade current constraints.

It could be that DM interacts with ordinary matter but not through a photon. Therefore in Fig. 3 we show upper limits on the DM-nucleon momentum-transfer cross section, for a variety of cross section dependences on relative velocity  $\sigma_{N\chi}(v_{\text{rel}}) = \sigma_{v_0}(v_{\text{rel}}/v_0)^n$ . The limits from Leo T are shown at  $v_0 = 10 \text{ km/s}$ , and those from G33.4–8.0 are shown at  $v_0 = 200 \text{ km/s}$ .  $n = -4$  arises for a massless mediator as in Rutherford scattering,  $n = \pm 2$  for DM having an electric and/or magnetic dipole moment [63]; while yukawa interaction produces more complex v-dependence not generally described by a simple power law [46]. For  $n = -4$ , Leo T gives the strongest limits on DM-baryon

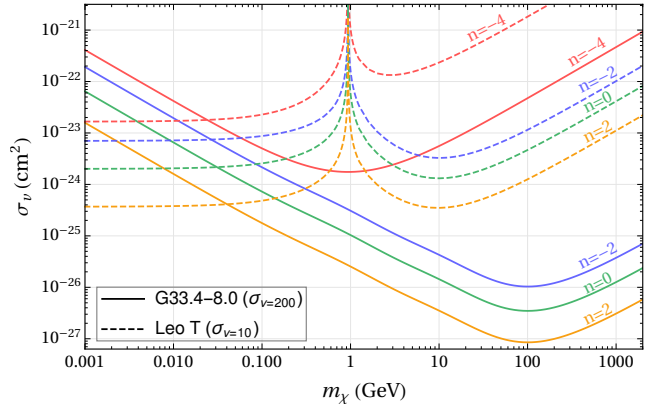


FIG. 3. Upper bounds on the DM-nucleon scattering cross-section from the gas temperature of the cloud G33.4–8.0 (solid) and Leo T (dashed), for velocity dependence  $\sigma_{N\chi}(v) = \sigma_{v_0}(v/v_0)^n$  for  $n = 0, \pm 2, -4$ . Note that the cross section limits are shown at different velocities, namely the typical values constrained by the systems ( $v_0 = 10 \text{ km/s}$  for Leo T and  $v_0 = 200 \text{ km/s}$  for the MW cloud).

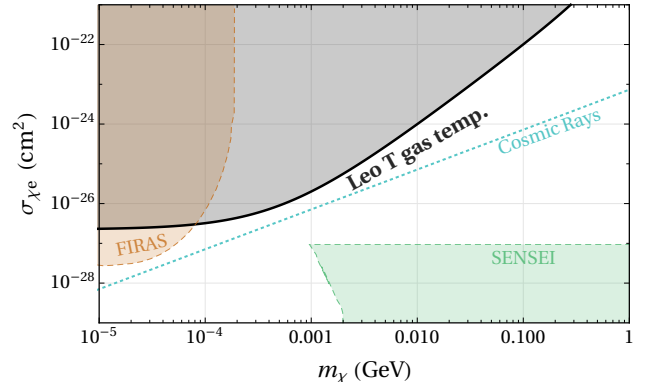


FIG. 4. Upper bounds on DM-free electron velocity independent scattering from Leo T (black), FIRAS (brown) [57] and indirect, model-dependent bounds from Cosmic Rays [58] (cyan). The exclusion region from SENSEI [48] is also shown.

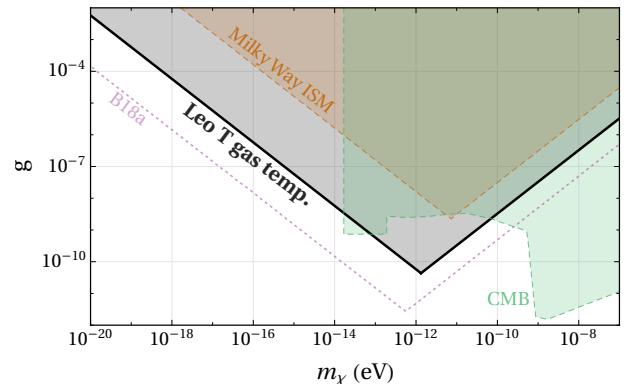


FIG. 5. Bounds on ultra-light dark photons with mass  $m_\chi$  and kinetic mixing parameter  $g$  from Leo T (black), heating of Milky Way's interstellar medium (ISM) (brown) [59] and CMB (green) [60, 61]. The (invalid) constraint reported by [62] based on HVNO clouds is shown by the purple dotted line.

cross section for  $m_\chi \lesssim 100$  MeV:  $\sigma_{v_0=c} < 1.5 \times 10^{-41}$  cm $^2$ . Leo T also gives new, direct constraints on velocity independent DM-electron interactions and on ultra-light dark photons as shown in Figs. 4 and 5 respectively; for details see SM [23].

## Summary

We have used the Leo T dwarf galaxy to exclude DM interactions over a large DM mass range, by requiring that DM-gas interactions transfer energy at a lower rate than the radiative cooling rate. These constraints are a valuable complement to CMB constraints and direct detection experiments since they *i*) directly probe much lower  $v_{\text{rel}}$  than previously tested, *ii*) are less sensitive to complex, novel and potentially inadequately understood semi-conductor physics (SENSEI), *iii*) avoid the problem for CSR and XQC that the efficiency of thermalization in the detectors has not yet been measured and may be very small [47] and *iv*) are independent of the uncertainties in the velocity distribution and number density of DM at Earth [64]. Leo T also sets new bounds on ultra-light dark photon mixing and on DM-electron interactions. We also present limits from robust Milky Way gas clouds, complementing Leo T with greater sensitivity to higher relative velocities.

We thank A. Sternberg, F. J. Lockman, C. McKee, M. S. Mahdawi, N. Outmezguine, E. Kovetz, C. Mondino, M. Muzio, K. Schutz, A. Maccio, M. Kulkarni, M. Baryakhtar and S. Dubovsky for useful discussions and Y. Faerman, X. Xu and M. S. Mahdawi for contributions to the plots. The research of GRF has been supported by NSF-PHY-1212538 and NSF-AST-1517319.

\* jay.wadekar@nyu.edu  
 † gf25@nyu.edu

[1] J. D. Bowman, A. E. E. Rogers, R. A. Monsalve, T. J. Mozdzen, and N. Mahesh, *Nature* **555**, 67 (2018).  
 [2] R. Barkana, *Nature* **555**, 71 (2018), arXiv:1803.06698 [astro-ph.CO].  
 [3] B. Holdom, *Phys. Lett.* **166B**, 196 (1986).  
 [4] D. A. Neufeld, G. R. Farrar, and C. F. McKee, *Astrophys. J.* **866**, 111 (2018), arXiv:1805.08794 [astro-ph.CO].  
 [5] E. V. Ryan-Weber, A. Begum, T. Oosterloo, S. Pal, M. J. Irwin, V. Belokurov, N. W. Evans, and D. B. Zucker, *MNRAS* **384**, 535 (2008), arXiv:0711.2979.  
 [6] J. D. Simon and M. Geha, *ApJ* **670**, 313 (2007), arXiv:0706.0516.  
 [7] E. A. K. Adams and T. A. Oosterloo, *A&A* **612**, A26 (2018), arXiv:1712.06636.  
 [8] S. L. Dubovsky, D. S. Gorbunov, and G. I. Rubtsov, *Soviet Journal of Experimental and Theoretical Physics Letters* **79**, 1 (2004), arXiv:hep-ph/0311189 [astro-ph].  
 [9] S. D. McDermott, H.-B. Yu, and K. M. Zurek, *Phys. Rev. D* **83**, 063509 (2011), arXiv:1011.2907 [hep-ph].  
 [10] K. K. Boddy, V. Gluscevic, V. Poulin, E. D. Kovetz, M. Kamionkowski, and R. Barkana, *Phys. Rev. D* **98**, 123506 (2018), arXiv:1808.00001 [astro-ph.CO].  
 [11] E. D. Kovetz, V. Poulin, V. Gluscevic, K. K. Boddy, R. Barkana, and M. Kamionkowski, *Phys. Rev. D* **98**, 103529 (2018), arXiv:1807.11482 [astro-ph.CO].  
 [12] W. L. Xu, C. Dvorkin, and A. Chael, *Phys. Rev. D* **97**, 103530 (2018), arXiv:1802.06788 [astro-ph.CO].  
 [13] T. R. Slatyer and C.-L. Wu, *Phys. Rev. D* **98**, 023013 (2018), arXiv:1803.09734 [astro-ph.CO].  
 [14] S. Davidson, S. Hannestad, and G. Raffelt, *Journal of High Energy Physics* **2000**, 003 (2000), arXiv:hep-ph/0001179 [hep-ph].  
 [15] A. Bhoonah, J. Bramante, F. Elahi, and S. Schon, *Phys. Rev. Lett.* **121**, 131101 (2018), arXiv:1806.06857 [hep-ph].  
 [16] N. M. McClure-Griffiths, J. A. Green, A. S. Hill, F. J. Lockman, J. M. Dickey, B. M. Gaensler, and A. J. Green, *ApJ* **770**, L4 (2013), arXiv:1304.7538.  
 [17] E. M. Di Teodoro, N. M. McClure-Griffiths, F. J. Lockman, S. R. Denbo, R. Endsley, H. A. Ford, and K. Harrington, *ApJ* **855**, 33 (2018), arXiv:1802.02152.  
 [18] J. L. Cooper, G. V. Bicknell, R. S. Sutherland, and J. Bland-Hawthorn, *ApJ* **674**, 157 (2008).  
 [19] E. Scannapieco and M. Brüggen, *ApJ* **805**, 158 (2015), arXiv:1503.06800 [astro-ph.GA].  
 [20] E. E. Schneider and B. E. Robertson, *ApJ* **834**, 144 (2017), arXiv:1607.01788 [astro-ph.GA].  
 [21] L. Armillotta, F. Fraternali, J. K. Werk, J. X. Prochaska, and F. Marinacci, *MNRAS* **470**, 114 (2017), arXiv:1608.05416 [astro-ph.GA].  
 [22] C. Melioli, E. M. de Gouveia Dal Pino, and F. G. Geraisate, *MNRAS* **430**, 3235 (2013), arXiv:1301.5005 [astro-ph.CO].  
 [23] See Supplemental Material (SM) which includes methods, data, additional analysis and Refs. [67-79].  
 [24] Y. Pidopryhora, F. J. Lockman, J. M. Dickey, and M. P. Rupen, *ApJS* **219**, 16 (2015), arXiv:1506.03873.  
 [25] B. D. Smith, G. L. Bryan, S. C. O. Glover, N. J. Goldbaum, M. J. Turk, J. Regan, J. H. Wise, H.-Y. Schive, T. Abel, A. Emerick, B. W. O'Shea, P. Anninos, C. B. Hummels, and S. Khochfar, *MNRAS* **466**, 2217 (2017), arXiv:1610.09591.  
 [26] E. N. Kirby, G. A. Lanfranchi, J. D. Simon, J. G. Cohen, and P. Guhathakurta, *ApJ* **727**, 78 (2011), arXiv:1011.4937 [astro-ph.GA].  
 [27] [65] studied the Hubble space telescope data for Leo T and found the isochronal metallicity of the gas [M/H] to be  $\sim -1.8$  to  $-1.6$ .  
 [28] Y. Faerman, A. Sternberg, and C. F. McKee, *Astrophys. J.* **777**, 119 (2013), arXiv:1309.0815 [astro-ph.CO].  
 [29] The more recent paper [30] introduces an iterative procedure for modeling the gas as non-isothermal using the spatially-resolved H $\alpha$  data of Leo T. However, the results of [30] are not sufficient for our purposes as [30] does not consider the gas ionization due to the metagalactic background [66]. This is needed for placing millicharged DM constraints and also required for properly interpreting the H $\alpha$  column density profile because the metagalactic background determines the transition from un-ionized (H $\alpha$ ) gas in the central region to ionized gas in the outer region.  
 [30] N. N. Patra, *MNRAS* **480**, 4369 (2018), arXiv:1802.04478.

[31] A. Begum, J. N. Chengalur, I. D. Karachentsev, S. S. Kaisin, and M. E. Sharina, *MNRAS* **365**, 1220 (2006), [astro-ph/0511253](#).

[32] There is also some amount of cold neutral medium at a much lower temperature ( $\sim$ 500K) present in the Leo T galaxy [5]; including it in our analysis might make our bounds stronger but the cold medium has not been observed with appropriate resolution to be able to model it, so we ignore it here.

[33] F. J. Lockman, *ApJ* **580**, L47 (2002), [astro-ph/0210424](#).

[34] H. A. Ford, N. M. McClure-Griffiths, F. J. Lockman, J. Bailin, M. R. Calabretta, P. M. W. Kalberla, T. Murphy, and D. J. Pisano, *ApJ* **688**, 290 (2008), [arXiv:0807.3550](#).

[35] H. A. Ford, F. J. Lockman, and N. M. McClure-Griffiths, *ApJ* **722**, 367 (2010), [arXiv:1008.2760](#).

[36] B. P. Wakker, *ApJS* **136**, 463 (2001), [astro-ph/0102147](#).

[37] P. Richter, K. R. Sembach, B. P. Wakker, B. D. Savage, T. M. Tripp, E. M. Murphy, P. M. W. Kalberla, and E. B. Jenkins, *ApJ* **559**, 318 (2001), [astro-ph/0105466](#).

[38] P. Richter, B. P. Wakker, B. D. Savage, and K. R. Sembach, *ApJ* **586**, 230 (2003), [astro-ph/0211356](#).

[39] K. R. Sembach, B. P. Wakker, T. M. Tripp, P. Richter, J. W. Kruk, W. P. Blair, H. W. Moos, B. D. Savage, J. M. Shull, D. G. York, G. Sonneborn, G. Hébrard, R. Ferlet, A. Vidal-Madjar, S. D. Friedman, and E. B. Jenkins, *ApJS* **150**, 387 (2004), [astro-ph/0311177](#).

[40] A. K. Hernandez, B. P. Wakker, R. A. Benjamin, D. French, J. Kerp, F. J. Lockman, S. O'Toole, and B. Winkel, *ApJ* **777**, 19 (2013), [arXiv:1308.6313](#) [astro-ph.GA].

[41] J. Bovy, *ApJS* **216**, 29 (2015), [arXiv:1412.3451](#).

[42] F. Nesti and P. Salucci, *Journal of Cosmology and Astro-Particle Physics* **2013**, 016 (2013), [arXiv:1304.5127](#) [astro-ph.GA].

[43] M. Hoeft, J. P. Mücke, and S. Gottlöber, *ApJ* **602**, 162 (2004), [arXiv:astro-ph/0311083](#) [astro-ph].

[44] U. Maio, K. Dolag, B. Ciardi, and L. Tornatore, *MNRAS* **379**, 963 (2007), [arXiv:0704.2182](#) [astro-ph].

[45] S. De Rijcke, J. Schroyen, B. Vandenbroucke, N. Jachowicz, J. Decroos, A. Cloet-Osselaer, and M. Koleva, *MNRAS* **433**, 3005 (2013), [arXiv:1306.4860](#).

[46] X. Xu and G. R. Farrar, in preparation (2019).

[47] M. S. Mahdawi and G. R. Farrar, *J. Cosmology Astropart. Phys.* **10**, 007 (2018), [arXiv:1804.03073](#) [hep-ph].

[48] M. Crisler, R. Essig, J. Estrada, G. Fernandez, J. Tiffenberg, M. S. Haro, T. Volansky, T.-T. Yu, and Sennsei Collaboration, *Phys. Rev. Lett.* **121**, 061803 (2018), [arXiv:1804.00088](#) [hep-ex].

[49] A. A. Prinz, R. Baggs, J. Ballam, S. Ecklund, C. Fertig, J. A. Jaros, K. Kase, A. Kulikov, W. G. J. Langeveld, R. Leonard, T. Marvin, T. Nakashima, W. R. Nelson, A. Odian, M. Pertsova, G. Putallaz, and A. Weinstein, *Phys. Rev. Lett.* **81**, 1175 (1998).

[50] R. Essig, A. Manalaysay, J. Mardon, P. Sorensen, and T. Volansky, *Phys. Rev. Lett.* **109**, 021301 (2012), [arXiv:1206.2644](#) [astro-ph.CO].

[51] R. Essig, T. Volansky, and T.-T. Yu, *Phys. Rev. D* **96**, 043017 (2017), [arXiv:1703.00910](#) [hep-ph].

[52] D. McCammon *et al.*, *Astrophys. J.* **576**, 188 (2002), [arXiv:astro-ph/0205012](#) [astro-ph].

[53] G. Angloher *et al.* (CRESST), *Eur. Phys. J.* **C77**, 637 (2017), [arXiv:1707.06749](#) [astro-ph.CO].

[54] A. Berlin, D. Hooper, G. Krnjaic, and S. D. McDermott, *Phys. Rev. Lett.* **121**, 011102 (2018), [arXiv:1803.02804](#) [hep-ph].

[55] R. Barkana, N. J. Outmezguine, D. Redigolo, and T. Volansky, *Phys. Rev.* **D98**, 103005 (2018), [arXiv:1803.03091](#) [hep-ph].

[56] J. B. Muoz and A. Loeb, *Nature* **557**, 684 (2018), [arXiv:1802.10094](#) [astro-ph.CO].

[57] Y. Ali-Haïmoud, J. Chluba, and M. Kamionkowski, *Phys. Rev. Lett.* **115**, 071304 (2015), [arXiv:1506.04745](#) [astro-ph.CO].

[58] C. V. Cappiello, K. C. Y. Ng, and J. F. Beacom, arXiv e-prints , [arXiv:1810.07705](#) (2018), [arXiv:1810.07705](#) [hep-ph].

[59] S. Dubovsky and G. Hernández-Chifflet, *Journal of Cosmology and Astro-Particle Physics* **2015**, 054 (2015), [arXiv:1509.00039](#) [hep-ph].

[60] P. Arias, D. Cadamuro, M. Goodsell, J. Jaeckel, J. Redondo, and A. Ringwald, *Journal of Cosmology and Astro-Particle Physics* **2012**, 013 (2012), [arXiv:1201.5902](#) [hep-ph].

[61] J. Jaeckel and A. Ringwald, *Annual Review of Nuclear and Particle Science* **60**, 405 (2010), [arXiv:1002.0329](#) [hep-ph].

[62] A. Bhoonah, J. Bramante, F. Elahi, and S. Schon, arXiv e-prints (2018), [arXiv:1812.10919](#) [hep-ph].

[63] K. Sigurdson, M. Doran, A. Kurylov, R. R. Caldwell, and M. Kamionkowski, *Phys. Rev. D* **70**, 083501 (2004), [astro-ph/0406355](#).

[64] L. Necib, M. Lisanti, and V. Belokurov, ArXiv e-prints (2018), [arXiv:1807.02519](#).

[65] D. R. Weisz, D. B. Zucker, A. E. Dolphin, N. F. Martin, J. T. A. de Jong, J. A. Holtzman, J. J. Dalcanton, K. M. Gilbert, B. F. Williams, E. F. Bell, V. Belokurov, and N. W. Evans, *ApJ* **748**, 88 (2012), [arXiv:1201.4859](#).

[66] F. Haardt and P. Madau, *ApJ* **746**, 125 (2012), [arXiv:1105.2039](#).

[67] N. M. McClure-Griffiths, J. M. Dickey, B. M. Gaensler, A. J. Green, J. A. Green, and M. Haverkorn, *ApJS* **199**, 12 (2012), online data at <http://www.atnf.csiro.au/research/HI/sgps/GalacticCenter/Data.html>, [arXiv:1201.2438](#).

[68] G. R. Farrar, F. J. Lockman, N. M. McClure-Griffiths, and D. S. Wadekar, *Phys. Rev. Lett., Comment*, submitted , (2019).

[69] G. J. Ferland, M. Chatzikos, F. Guzmán, M. L. Lykins, P. A. M. van Hoof, R. J. R. Williams, N. P. Abel, N. R. Badnell, F. P. Keenan, R. L. Porter, and P. C. Stancil, *Rev. Mexicana Astron. Astrofis.* **53**, 385 (2017), [arXiv:1705.10877](#) [astro-ph.GA].

[70] A. Rahmati, A. H. Pawlik, M. Raičević, and J. Schaye, *MNRAS* **430**, 2427 (2013), [arXiv:1210.7808](#) [astro-ph.CO].

[71] R. Kannan *et al.*, *Mon. Not. Roy. Astron. Soc.* **437**, 2882 (2014), [arXiv:1310.6748](#) [astro-ph.GA].

[72] M. G. Wolfire, C. F. McKee, D. Hollenbach, and A. G. G. M. Tielens, *ApJ* **587**, 278 (2003), [arXiv:astro-ph/0207098](#) [astro-ph].

[73] C. Dvorkin, T. Lin, and K. Schutz, arXiv e-prints , [arXiv:1902.08623](#) (2019), [arXiv:1902.08623](#) [hep-ph].

[74] G. G. Raffelt, *Phys. Rev. D* **33**, 897 (1986).

[75] C. Kouvaris and I. M. Shoemaker, *Phys. Rev. D* **90**, 095011 (2014), [arXiv:1405.1729](#) [hep-ph].

[76] R. H. Helm, *Phys. Rev.* **104**, 1466 (1956).

[77] C. Dvorkin, K. Blum, and M. Kamionkowski,

Phys. Rev. D **89**, 023519 (2014), arXiv:1311.2937.  
 [78] K. Lodders, *Astrophysics and Space Science Proceedings* **16**, 379 (2010), arXiv:1010.2746 [astro-ph.SR].  
 [79] J. B. Muñoz, E. D. Kovetz, and Y. Ali-Haïmoud,

Phys. Rev. D **92**, 083528 (2015), arXiv:1509.00029.

## Supplemental Material for ‘First direct astrophysical constraints on dark matter interactions with ordinary matter at very low velocities’

### I. Milky Way gas clouds

In the main text we reported the best robust constraints on DM-gas interactions using Milky Way (MW) gas cloud cooling rates, based on G33.4–8.0. In this section we discuss other clouds in addition to G33.4–8.0 which we have considered. The parameters for the most relevant clouds are reported in Table S1. For the parameters reported with error bars, we use the central values for calculating our results.

Among the clouds in [24] which co-rotate with the MW disk and are therefore potentially long-lived, the cores of G26.9–6.3 and G16.0+3.0 give the next best constraints after G33.4–8.0. For all three cloud cores, the radiative cooling time ( $\tau_{\text{cool}} \lesssim 0.7$  Myr) is much smaller than the free-fall or dynamical time-scale ( $\tau_{\text{dynamic}} \sim 20–50$  Myr) [24]. Therefore the cores can be taken to be in thermal equilibrium. The constraints on DM obtained from these clouds are shown in Fig. S2.

*HVNO clouds*— Compared to the co-rotating clouds, one could potentially obtain stronger constraints on DM using clouds which are near the Galactic center where the DM density is higher. A number of clouds entrained in the high velocity nuclear outflow (HVNO) originating in the Galactic center were discovered in HI data from the Australia Telescope Compact Array (ATCA) and the Green Bank Telescope (GBT) [16, 17]. Ref. [15] (B18) used the cloud G1.4–1.8+87 reported in [16] to constrain millicharge DM, but with incorrect parameters for the cloud. Correct parameters are listed in Table S1. The temperature of G1.4–1.8+87 quoted in Table S1 is determined by fitting the public online HI brightness temperature spectrum data from [67], shown in the top panel of Fig. S1. For comparison, the spectrum of the co-rotating cloud G33.4–8.0 used in our analysis, is shown in the bottom panel of Fig. S1.

Correcting the parameters of G1.4–1.8+87, one finds that among the HVNO clouds, G357.6–4.7–55 and G355.3–3.3–118 would yield the strongest constraints. If the use of HVNO clouds for constraining DM were valid, the corresponding limits would be those shown by the thin solid cyan and grey lines in Fig. S2. We also show for comparison, the limits reported by B18 based on incorrect parameters for G1.4–1.8+87. The correct limits on the DM cross-section derived from that cloud are a factor  $\sim 10^6$  weaker than reported by B18; for further details see [68].

TABLE S1. Parameters for all the analyzed clouds

Cloud Name	$n$ ( $\text{cm}^{-3}$ )	T (K)	$R$ (kpc)	$ z $ (kpc)
G33.4–8.0	$0.4 \pm 0.1$	$400 \pm 90$	$4.68 \pm 0.41$	$1 \pm 0.28$
G16.0+3.0	$1.7 \pm 0.2$	$480 \pm 20$	$2.34 \pm 0.2$	$0.43 \pm 0.05$
G26.9–6.3	$2.5 \pm 0.5$	$200 \pm 13$	$3.85 \pm 0.36$	$0.84 \pm 0.19$
G357.6–4.7–55 <sup>a</sup>	0.43	136.4	0.36	0.70
G355.3–3.3–118 <sup>a</sup>	0.24	366.8	0.72	0.48
G1.4–1.8–87 <sup>a</sup>	0.3	15441 <sup>b</sup>	0.24	0.27

<sup>a</sup> Clouds in the Galactic high velocity nuclear outflow.

<sup>b</sup> B18 uses the incorrect value 22 K for the temperature of G1.4–1.8+87, while the correct value is 15441 K.

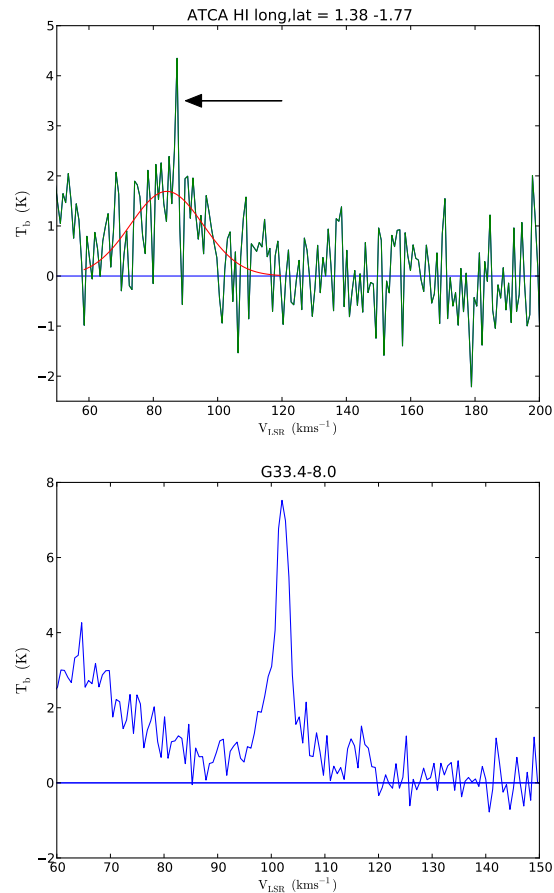


FIG. S1. *Top*: The HI brightness temperature spectrum in the direction of G1.4–1.8+87. An arrow marks the extremely narrow line quoted in the McG13 table, while the smooth curve shows a Gaussian fit to the emission feature. *Bottom*: The corresponding spectrum for G33.4–8.0 [24]. Figures and fit courtesy F. J. Lockman.

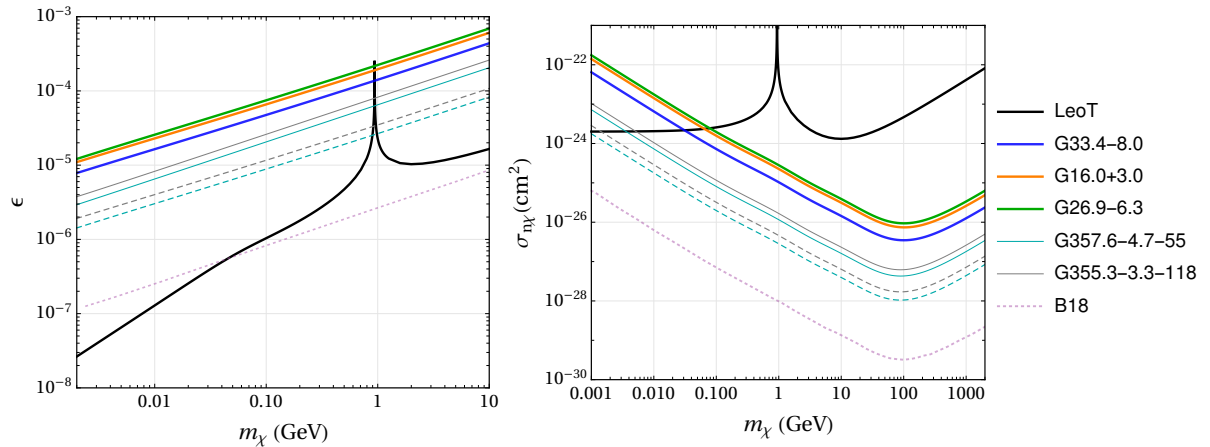


FIG. S2. Limits on  $\epsilon$  (left panel) and the DM-nucleon velocity independent cross-section  $\sigma_{n\tilde{\chi}}$  (right panel). The bound from Leo T is shown in black and the bounds from the three best co-rotating MW gas clouds are shown as solid blue, orange, and green lines. The bounds from the two best Galactic high velocity nuclear outflow clouds are shown as thin cyan and gray lines, where the solid lines are the bounds when the best fit Burkert profile from [42] is used for the DM halo and the dashed lines when the NFW profile from [41] is used. For the co-rotating clouds, the change in bounds when the Burkert profile is used instead of NFW is insignificant. The dotted line is the bound claimed by B18. Solar metallicity is assumed for all the clouds.

The limits shown in Fig. S2 are obtained assuming a uniform density profile for the clouds of [16, 17] and taking the clouds to be moving radially outward from the Galactic center with a speed of  $\sim 330$  km/s, as inferred from simulations of the ensemble of clouds performed by [17]. Following [17], we deduce the 3D position of the cloud using the cloud's latitude and longitude, its radial velocity following the HVNO flow [17], and the individual cloud's line-of-sight velocity toward the local standard of rest,  $v_{\text{LSR}}$ . We give the cylindrical radial distance  $R$  from the Galactic center and height  $z$  from the disk in Table S1.

So close to the Galactic center, the DM density is quite uncertain. An isothermal core is more plausible than the NFW cusp. We adopt a recent parameterization of the Burkert profile  $\rho_\chi = \rho_B / [(1 + r/r_B)(1 + r^2/r_B^2)]$  by [42] with the core radius  $r_B \sim 9.26$  kpc and the central density  $\rho_B \sim 1.57$  GeV/cm $^3$ . Assuming an NFW profile would give stronger constraints shown by the dashed grey and cyan lines in Fig. S2, but would be neither well-motivated nor conservative.

However, there is strong reason to be skeptical about the general strategy of deriving thermal equilibrium bounds on DM from the HVNO clouds because such analysis requires the clouds to be stable at their current temperature over the long timescales associated with their radiative cooling rate. Being entrained in a high velocity, presumably turbulent wind, such clouds are subject to shocks due to Kelvin-Helmholtz instabilities, surface ablation and evaporation, hydrodynamic drag force and ram pressure due to the hot wind [18–22].

The radiative cooling timescale of G357.6–4.7–55 and G355.3–3.3–118 is  $\sim 1$  Myr. For a cloud of density  $n_c$

and radius  $r_c$  entrained in a wind with a density  $\rho_w$ , velocity  $V_w$  and temperature  $T_w$ , the cloud crushing time [18] is  $t_{\text{cr}} = \rho_c r_c / \rho_w V_w \sim 1$  Myr for the two best HVNO clouds we consider, based on the hydrodynamical models of the wind in [16] ( $n_w \sim 10^{-2}$  cm $^{-3}$  and  $T_w \sim 10^{6–7}$  K). Furthermore, for clouds entrained in a high-velocity hot wind, shocks occur on their surface at the temperature  $T_{\text{cl,sh}} = 3/16 T_w (n_w/n_c)$  [18]. The cooling time of such shocked regions on the cloud surface is on the order of a few hundred years [16, 18]. The shock cooling time is short compared to the cloud-shock crossing time, potentially causing the radiative shock driven into the cloud to form a high-density shell which might prevent further disruption [18]. Thus the long-term stability of the HVNO clouds is subject to great uncertainty.

Note that the simple Cloudy [69] simulation of the HVNO clouds in [62], which ignores the effects of the hot, high-velocity wind in the environment on the clouds and assumes a nearly-uniform density profile for the clouds, therefore cannot be expected to accurately model the cloud properties.

## II. Astrophysical heating and cooling processes

*Radiative cooling*— For calculating the radiative cooling rate of HI gas, we use the chemistry and radiative cooling library for astrophysical simulations called Grackle [25]. It allows us to include metal cooling and other collisional cooling effects and to take into account the ionization due to the metagalactic background [66] and the self-shielding from the UV background [70]. The cooling function  $\Lambda(T)$  for a gas with solar metallicity is

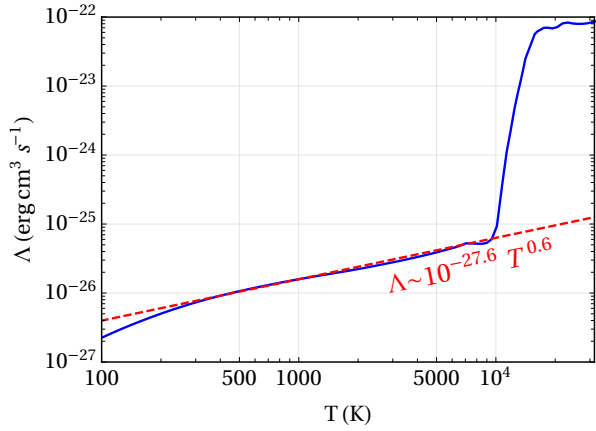


FIG. S3. The radiative cooling function from [25] for HI gas with solar metallicity (solid blue line). A convenient approximation for the cooling function  $\Lambda(T) = 10^{-27.6} T^{0.6}$  for  $T \sim (300 - 8000)$  K is shown as the dashed line.

shown in Fig. S3. For solar metallicity gas within the parameter domain  $T \sim (300 - 8000)$  K and  $n_{\text{H}} \sim (0.1 - 10^3)$  cm<sup>-3</sup>, the dominant contribution to radiative cooling comes from the fine structure transitions of oxygen, carbon, silicon and iron [44]. An approximation which we found applicable over most of the range of the cooling curve is also shown; it is convenient for quickly assessing a cloud's likely utility for constraining DM interactions (roughly speaking the product  $n_{\text{H}} \times 10^{[\text{Fe}/\text{H}]} \times T^{0.6}$  should be minimized for best constraints). Note that we use the exact, solid curve from [25] in our analysis for obtaining limits on DM interactions.

*Astrophysical heating*— UV radiation from the metal-galactic background [66] and radiation from stars causes photo-ionization heating in Leo T and MW gas clouds [71]. A substantial contribution to the heating of the MW clouds comes from photo-ejection of electrons due to UV radiation impinging on dust [72]. The dust content of the MW clouds is quite uncertain but can easily span the range required to balance the calculated cooling rate. If we include astrophysical heating in our calculation of thermal equilibrium DM bounds, we should get stronger bounds on DM interactions.

### III. Momentum-transfer cross-sections employed

We consider the following scenarios in which a DM particle interacts with the astrophysical systems; a formula for the transfer cross-section for each of them is given below.

*Charged DM interacting with plasma*— For a DM particle interacting with a charged particle  $i$  present in the plasma, the differential Rutherford scattering cross sec-

tion is

$$\frac{d\sigma_{i\chi}}{d\Omega_{\text{CM}}} = \frac{Z_i^2 \alpha_{\text{em}}^2 \epsilon^2}{4\mu_i^2 v_{\text{rel}}^4 \sin^4(\theta_{\text{CM}}/2)}, \quad (\text{S1})$$

where  $\mu_i$  is the DM-particle reduced mass,  $Z_i$  is the particle charge,  $n_i$  is the number density and  $\theta_{\text{CM}}$  is the scattering angle in the center of mass frame. The ions in a thermal plasma are screened at distances greater than the Debye length

$$\lambda_D = \sqrt{\frac{T}{4\alpha_{\text{em}}\pi(\sum_i Z_i^2 n_i)}}. \quad (\text{S2})$$

The momentum-transfer cross-section (defined in the first equality) is

$$\begin{aligned} \sigma_{i\chi}^T(v) &\equiv \int_{\Omega_{\text{CM}}^{\min}} d\Omega_{\text{CM}} \frac{d\sigma_{i\chi}}{d\Omega_{\text{CM}}} (1 - \cos \theta_{\text{CM}}) \\ &= \frac{4\pi Z_i^2 \alpha_{\text{em}}^2 \epsilon^2}{\mu_i^2 v_{\text{rel}}^4} \ln\left(\frac{2\mu_i v_{\text{rel}}}{1/\lambda_D}\right), \end{aligned} \quad (\text{S3})$$

where the angular integral is cut-off when the scattering angle becomes the Debye angle  $\theta_{\text{CM}}^{\min} = 1/(\lambda_D \mu_i v_{\text{rel}})$  for a non-relativistic plasma [8, 14, 73, 74].

*Charged DM interacting with neutral atoms*— Following [75], we use the screened Coulomb potential ( $V = q_1 q_2 e^{-r/a}/r$ , where  $q_{1,2}$  are the charges on DM and the nucleus) for incorporating the effect of screening. The nucleus  $A$  is screened at distances greater than the Thomas-Fermi radius  $a = 0.8853 a_0/Z_A^{1/3}$ , where  $a_0$  is the Bohr radius and the differential DM-nucleus cross section is

$$\frac{d\sigma_{A\chi}}{dE_{\text{nr}}} = \frac{8\pi \alpha_{\text{em}}^2 \epsilon^2 Z_A^2 m_A a^4}{v^2 (2a^2 m_A E_{\text{nr}} + 1)^2}, \quad (\text{S4})$$

where  $E_{\text{nr}}$  is the nuclear recoil energy. Therefore,

$$\begin{aligned} \sigma_{A\chi}^T(v) &\equiv \int_0^{E_{\text{nr}}^{\max}} dE_{\text{nr}} \frac{d\sigma_A}{dE_{\text{nr}}} (1 - \cos \theta_{\text{CM}}) \\ &= \frac{2\pi \alpha_{\text{em}}^2 \epsilon^2 Z_A^2}{\mu_A^2 v_{\text{rel}}^4} \left[ \ln(1 + 4\mu_A^2 v_{\text{rel}}^2 a^2) - \frac{1}{1 + (4\mu_A^2 v_{\text{rel}}^2 a^2)^{-1}} \right], \end{aligned} \quad (\text{S5})$$

where  $E_{\text{nr}}^{\max} = (2\mu_A v)^2/2m_A$  is the maximum possible recoil energy. A more refined way of treating the electron screening would be to use the form factor of the electron cloud surrounding the nucleus but we adopt Eq. (S5) in this paper. Although the cross-section in Eq. (S3) for charged DM interacting with ions/electrons is higher than that of neutral atoms, the number density of neutral atoms in Leo T is much greater than that of electrons or ions in Region-I so neutral atom interactions with DM must be included alongside interactions with ions/electrons in Leo T.

*DM-baryon interactions*— For general interactions of DM with nucleus  $A$ , we consider the momentum-transfer

cross-section has a power law dependence of the form  $\sigma_{i\chi}^T(v_{\text{rel}}) = \sigma_0 v_{\text{rel}}^n$  where  $v_{\text{rel}}$  is the velocity of DM relative to baryons in units of  $c$ . For  $n = -4$ , we assume the interaction is Coulomb-like so the DM-nucleon cross-section scales similar to Eq. (S1), so

$$\sigma_{A\chi} \simeq \left( \frac{Z_A \mu_H}{Z_H \mu_A} \right)^2 \sigma_{\chi H}, \quad (\text{S6})$$

where  $Z$  is the atomic number. However, for  $n \in \{-2, 0, 2\}$ , we assume a heavy mediator for DM-nucleon interaction and the cross-section in Born approximation is given by

$$\sigma_{A\chi} = \sigma_{N\chi} \left( \frac{\mu_A}{\mu_p} \right)^2 A^2 F_A^2(E_{\text{nr}}). \quad (\text{S7})$$

We adopt the nuclear form factor proposed by [76]

$$F_A(E_{\text{nr}}) = 3 \left( \frac{\sin(qr_A) - qr_A \cos(qr_A)}{(qr_A)^3} \right) e^{-s^2 q^2/2}, \quad (\text{S8})$$

where  $q = \sqrt{2m_A E_{\text{nr}}}$  is the momentum transfer and  $r_A$  is the effective nuclear radius given by  $r_A^2 = c^2 + \frac{7}{3}\pi^2 a^2 - 5s^2$  with parameters  $c \simeq (1.23A^{1/3} - 0.6)$  fm,  $a \simeq 0.52$  fm and  $s = 0.9$  fm. We have neglected the nuclear form factor in Coulomb-like scattering due to smallness of the momentum transfer.

#### IV. DM heat exchange rate

We compute the DM heat exchange rate for momentum-transfer cross sections approximately having the form  $\sigma_{i\chi}^T(v_{\text{rel}}) = \sigma_0 v_{\text{rel}}^n$ . This is consistent with the charged DM scenario (Eqs. (S3) and (S5)) because we can ignore the  $v_{\text{rel}}$  dependence in the argument of the logarithm to a good approximation. We therefore replace  $v_{\text{rel}}$  in the argument of logarithms in Eqs. (S3) and (S5) by an average value when computing the heat exchange rate. The mechanism for DM heating of plasma for ultra-light dark photon dark matter is different and will be considered in section V separately.

Leo T— In Leo T, both DM and a component  $i$  of the gas have Maxwell-Boltzmann velocity distributions corresponding to their temperatures  $T_\chi$  and  $T_i$  respectively. Energy is exchanged between them if  $T_i \neq T_\chi$ . For the case when there is no relative bulk velocity between gas and DM (as is the case for Leo T), the rate of energy transfer to a component  $i$  of the gas per unit time per unit volume is [77]

$$\dot{Q}_i = \frac{2^{\frac{n+5}{2}} \Gamma(3 + \frac{n}{2})}{\sqrt{\pi} (m_i + m_\chi)^2} \rho_i \rho_\chi \sigma_0 (T_\chi - T_i) u_{\text{th}}^{n+1}, \quad (\text{S9})$$

where  $u_{\text{th}}^2 = T_\chi/m_\chi + T_i/m_i$  is the thermal sound speed of the DM-target fluid.

MW gas clouds— Treatment of heat exchange in gas clouds is different than for Leo T because, in addition to gas and DM being at different temperatures, they also have a non-zero relative bulk velocity between them. This bulk motion causes heating of gas and DM even if  $T_g = T_\chi$ . The energy transferred to a particle  $i$  in the cloud by a DM collision is  $E_T = \mu_{i\chi}^2 v_{\text{rel}}^2 (1 - \theta_{\text{CM}})/m_i$ , where  $\theta_{\text{CM}}$  is again the scattering angle in the center of mass frame.

For the millicharged case, using the cross-sections from Eqs. (S3) & (S5), the rate of energy transfer to an OM particle of type  $i$  as a result of a DM interactions becomes  $\dot{Q}_i \propto Z_i^2/m_i$ . Therefore free electrons make the dominant contribution towards the energy exchange with millicharged DM in the MW gas clouds. The gas heating scales linearly with the free electron density and thus linearly with the cloud metal fraction. Because the radiative cooling rate also scales linearly with the metal fraction, the bounds on millicharged DM are not affected by the cloud metallicity. Additional ionization in the gas clouds due to cosmic ray scattering, dust and UV radiation from stars should also increase the heating and cooling rate together and therefore their inclusion should not have a significant effect on the millicharge DM bounds from clouds.

The gas clouds that we have considered have low temperatures  $T_g \lesssim 500$  K, which means that the velocity dispersion of atoms or ions in the clouds is  $v \lesssim 2$  km/s which is much less than the relative bulk velocity  $V_{\chi i}$  between DM and the cloud ( $V_{\chi i}$  is 220 and 330 km/s for the co-rotating and the HVNO clouds respectively). Thus we can neglect the velocity dispersion to make the following simplification when computing the heat exchange when DM scatters with nuclei or ions in the clouds:

$$\begin{aligned} \dot{Q}_A &= \int d^3 v_A f(v_A) \int d^3 v_\chi f(v_\chi) n_p n_\chi \frac{\mu_A^2}{m_A} \sigma_0 v_{\text{rel}}^{n+3} \\ &\simeq \int d^3 v_\chi f(v_\chi) n_p n_\chi \frac{\mu_A^2}{m_A} \sigma_0 v_{\text{rel}}^{n+3}. \end{aligned} \quad (\text{S10})$$

For DM nucleon scattering in the case  $n = -4$ , metals in MW clouds have negligible contribution to DM heating whereas for  $n \in \{-2, 0, 2\}$ , metals in the MW clouds contribute dominantly to the DM heating for  $m_\chi \gtrsim 10$  GeV. The bounds on DM nucleon cross-sections for  $n \in \{-2, 0, 2\}$  &  $m_\chi \gtrsim 10$  GeV are independent of the cloud metallicity because both the radiative cooling rate and DM heating scale linearly with the metal fraction. While for the remaining cases ( $n = -4$  or  $m_\chi \lesssim 10$  GeV) the bounds would change by a factor  $10^{[\text{Fe}/\text{H}]}$  for metallicity different from solar (not expected). The solar

mass fractions for various elements are taken from [78]

$$\begin{aligned} r_A &= [r_H, r_{He}, r_O, r_C, r_{Ne}, r_{Fe}, r_{Si}] \\ &= [0.739, 0.2469, 0.0063, 0.0022, 0.0017, 0.0012, 0.0007]. \end{aligned} \quad (\text{S11})$$

For the case when DM scatters with electrons via Coulomb scattering ( $n = -4$ ), the velocity dispersion of free electrons  $v \lesssim 90$  km/s cannot be neglected as compared to the relative bulk velocity. In such a case we need to generalize Eq. (S9) to include the drag force between gas and DM alongside their thermal velocity distributions. Such a generalized form of Eq. (S9) for the  $n = -4$  case is [79]:

$$\begin{aligned} \dot{Q}_i &= \frac{\rho_i \rho_\chi \sigma_0}{(m_\chi + m_i)^2 u_{\text{th}}} \left[ \sqrt{\frac{2}{\pi}} \left( \frac{T_\chi - T_i}{u_{\text{th}}^2} - m_\chi \right) \exp \left( -\frac{1}{2} \frac{V_{\chi i}^2}{u_{\text{th}}^2} \right) \right. \\ &\quad \left. + m_\chi \frac{u_{\text{th}}}{V_{\chi i}} \text{Erf} \left( \frac{V_{\chi i}}{\sqrt{2} u_{\text{th}}} \right) \right], \end{aligned} \quad (\text{S12})$$

where  $u_{\text{th}}^2 = T_\chi/m_\chi + T_i/m_i$  is the same thermal sound speed of the DM-target fluid as defined earlier.

## V. Ultra-light dark photon DM

Here we consider the case that DM is made up only of vector bosons known as dark photons and no additional light particles carrying a charge are present. Following the formalism and conventions of [59], we calculate the heating in Leo T galaxy due to dark photons in the ultra-light regime  $m_\chi \lesssim 10^{-11}$  eV. We only show the relevant steps of the calculation in this section and encourage the reader to refer to [59] for further details. We consider that the dark photon is kinematically mixed with the standard model photon and the coupling strength is determined by a dimensionless parameter  $g$ . The resulting Lagrangian

is

$$\begin{aligned} \mathcal{L} &= -\frac{1}{4} F_{\mu\nu} F^{\mu\nu} - \frac{1}{4} \tilde{F}_{\mu\nu} \tilde{F}^{\mu\nu} + \frac{m_\chi^2}{2} \tilde{A}_\mu \tilde{A}^\mu \\ &\quad - \frac{e}{(1+g^2)^{1/2}} J^\mu \left( A_\mu + g \tilde{A}_\mu \right), \end{aligned} \quad (\text{S13})$$

where  $A_\mu$  ( $\tilde{A}_\mu$ ) and  $F_{\mu\nu}$  ( $\tilde{F}_{\mu\nu}$ ) stand for the visible (dark) photon gauge fields and field strengths respectively. As discussed in the main text, some part of Leo T is ionized due to the penetrating metagalactic X-ray background [66] and acts as a non-relativistic plasma, with the plasma frequency being

$$w_p = \sqrt{\frac{4\pi n_e \alpha}{m_e}}, \quad (\text{S14})$$

where  $n_e$  is the number density of electrons. Very light dark photons produce an oscillating electric field which induces an electric current in the ionized plasma in Leo T. The induced current is dissipated because the free electrons which are accelerated by the oscillating electric field collide with ions. The frequency  $\nu$  of electron-ion collisions is given by

$$\nu = \frac{4\sqrt{2\pi}\alpha^2 n_e}{3m_e^{1/2} T_e^{3/2}} \ln \Lambda_C, \quad (\text{S15})$$

where  $T_e$  is the electron temperature and the Coulomb logarithm is  $\ln \Lambda_C = 0.5 \log[4\pi T_e^3 / (\alpha^3 n_e)]$ . Due to the electron-ion collisions in the plasma, the dark photon potential energy is transformed into the kinetic energy of charged particles in Leo T and the resulting heating rate of the gas in Leo T per unit volume is given by

$$\dot{Q} = 2|\gamma_h| \rho_\chi, \quad (\text{S16})$$

where  $\rho_\chi$  is the dark photon gravitational energy density in  $\text{GeV/cm}^{-3}$  and  $\gamma_h$  is the imaginary part of the frequency of the dark photon modes ( $w = w_h + i\gamma_h$ ) and is given by

$$\gamma_h = \begin{cases} -\nu \frac{m_\chi^2}{2\omega_p^2} \frac{g^2}{1+g^2} & \text{for } m_\chi \ll \omega_p \\ -\nu \frac{\omega_p^2}{2m_\chi^2} \frac{g^2}{1+g^2} & \text{for } m_\chi \gg \omega_p. \end{cases} \quad (\text{S17})$$